Satellite Multispectral and Infrared Imagery Analysis to Contextualize Bridge Structural Health Observations – A study of the Samuel de Champlain Bridge in Montreal, Canada

HELEN STEWART and DANIEL CUSSON

ABSTRACT

In 2021-2022, two related validation studies were conducted on structural health monitoring of the Samuel de Champlain Bridge in the La Prairie Basin of the Saint Lawrence River near Montreal, Canada. In the first study, C-band satellite Interferometric Synthetic Aperture Radar (InSAR) observations of bridge line-of-sight thermal displacement measurements were compared to predicted values. A companion observational study of multispectral (MS) imagery assessed turbulent and flow features on the river's surface that are indicative of changes in the riverbed morphology and used stereo MS imagery to derive river velocity vectors using a Particle Image Velocimetry (PIV) algorithm.

This paper presents the preliminary findings of a follow-up study, in which time-series of InSAR displacement observations at nine piers of the Samuel de Champlain Bridge were compared to water depth, ambient water surface temperature from satellite imagery, and ambient air temperature from a nearby in-situ weather station.

INTRODUCTION

Background

North America has a significant amount of aging public infrastructure that is in poor condition. Structural health monitoring (SHM) provides a means for ensuring structural integrity and public safety, detecting damage accumulation, and estimating the performance of infrastructure assets over time. The National Research Council Canada and Fugro USA Marine have collaborated to combine innovative remote sensing technologies to assess bridge deformation and stability with radar satellite imagery [1] and turbulent flow features around river bridge piers with multispectral satellite imagery [2] in order to allow an overall assessment of several interrelated structural and environmental factors that may affect bridges' structural integrity. A follow-up study is presented in this paper.

Helen Stewart, Fugro USA Marine, 6100 Hillcroft Ave Houston, USA, 77011
Daniel Cusson, National Research Council Canada, 1200 Montreal Road, Ottawa, Canada, K1A 0R6

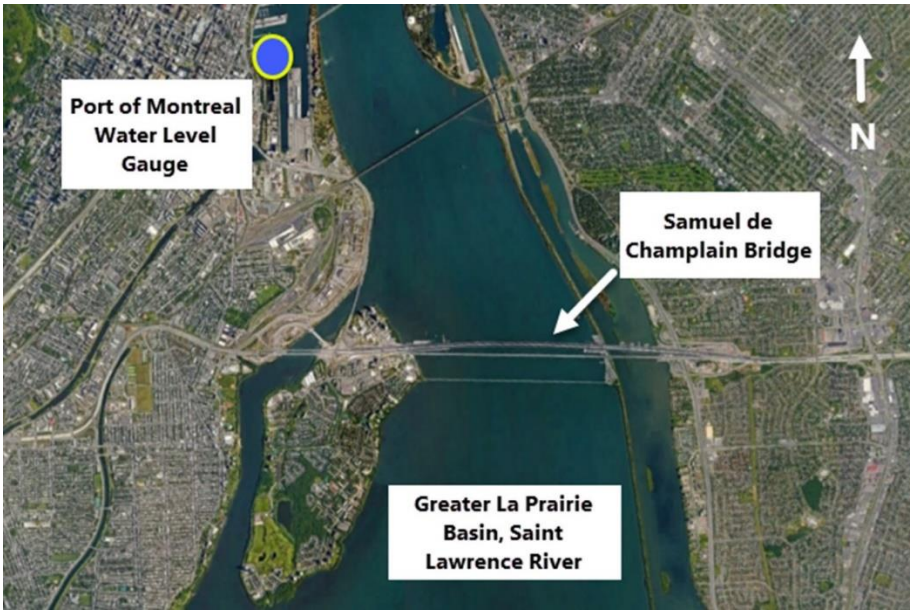

Figure 1. New Samuel de Champlain Bridge spanning the Greater La Prairie Basin of the Saint Lawrence River in Montreal, Canada.

Study Area

The study area comprises the Samuel de Champlain Bridge, which spans the Greater La Prairie Basin of the Saint Lawrence River in Montreal, Canada. The basin is a naturally occurring widening of the Saint Lawrence River characterized by shallow, rocky subsurface ledges, strong currents, and minimal ice cover in winter months. An artificial levee with locks separates the Greater La Prairie Basin from the Saint Lawrence Seaway shipping channel and the shallow, slow-flowing Lesser La Prairie Basin.

The newly constructed Samuel de Champlain Bridge – a large multi-transportation-mode bridge – spans the La Prairie Basin from its west abutment on Nun's Island to the Main Span Tower located on the levee separating the Greater La Prairie Basin from the Saint Lawrence Seaway to the east (Figure 1). While there are piers located to the east of the Main Span Tower, they are not considered in this study.

METHODS

Pier Selection

A total of 9 piers on the Samuel de Champlain Bridge were chosen to encompass a representative sample of river conditions (Figure 2). For instance, Pier W-17 on the Samuel de Champlain Bridge is located in the river thalweg, where current speeds may exceed 2 m/s. Piers W-02, W-23, and W-26 are in shallow water with low river flow and are surrounded by landfast ice in the winter months. The remaining piers were chosen to represent a range of water depths at Low Water Datum. The West Abutment (WA) of the bridge is wholly located over land and used as control.

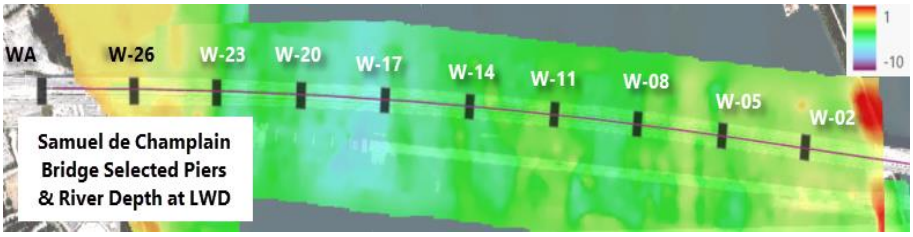

Figure 2. Selected Piers of the Samuel de Champlain Bridge. Also shown is the historical bathymetry from pre-construction and navigation surveys.

River Depth and Current Flow

Water depths at the bridge piers are relative to Low Water Datum (LWD) at the Port of Montreal and were acquired with a multibeam echosounder as part of the pre-construction environmental baseline survey conducted by Dessau-Cima+ and with singlebeam echosounder surveys by the Canadian Hydrographic Service. Soundings were used to build a triangular irregular network (TIN) at 3-meter resolution and minimally smoothed to create a bathymetric digital terrain model (DTM) of the Greater La Prairie Basin. Total estimated water depths (from the natural river bottom to the top of the water's surface) were computed by adding the water depth at each pier from the bathymetric DTM to the water level recorded at the Montréal Jetée No. 1 gauge, which is operated by the Canadian Hydrographic Service (CHS). Figure 3 shows the results.

River flow at each pier is estimated as either high flow or low flow according to water depth relative to LWD. In the 2021-2022 study [2], particle image velocimetry (PIV) of satellite imagery and classification of turbulent wakes downstream of bridge piers determined that where piers are located in depths less than 3 m LWD, current speeds are less than 0.5 m/s. Piers W-02 and W-26 of the Samuel de Champlain Bridge are classified as low-flow, while Pier W-05 in 3.5 m depth LWD is classified as seasonally low-flow because it is located adjacent to a naturally-occurring channel between two rocky ridges and current speeds in the channel may exceed 0.5 m/s during the spring runoff period. All other selected piers are classified as high flow.

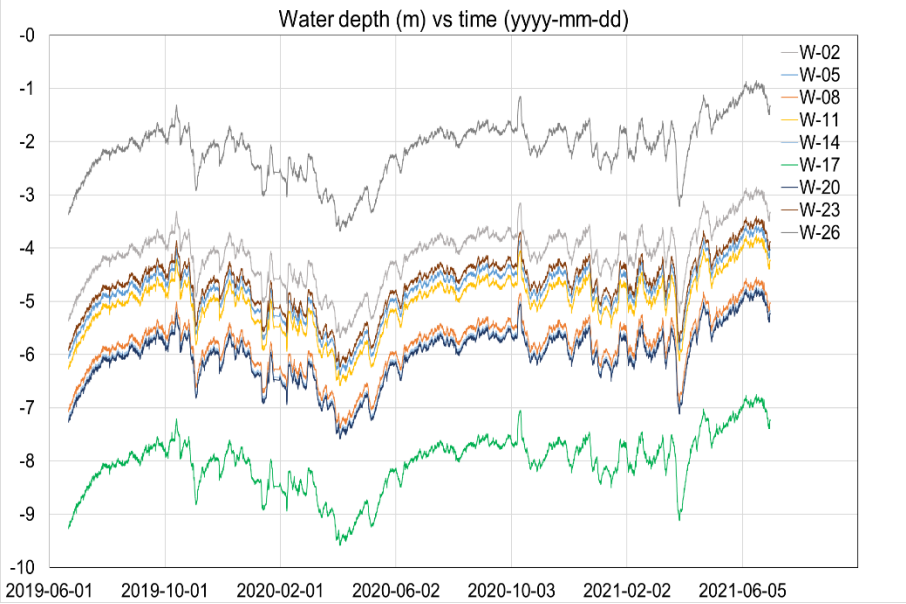

Figure 3. Total water depth (LWD datum depth + gauge depth) for each selected pier over time.

Water and Land Surface Temperature

River surface temperatures adjacent to the selected bridge piers were obtained using the Thermal InfraRed Sensor (TIRS) Band 10 on the Landsat-8 (2019–2022) and Landsat-9 (2022 only) satellites. The Landsat-8 and Landsat-9 satellites, operated by the U.S. Geological Survey (USGS), operate in a sun-synchronous orbit with a repeat cycle of 16 days. The TIRS instrument Band 10 observes skin-of-the-earth and skin-of-the-water temperature in the wavelength of 10.30–11.30 μm (long-wave infrared) at a native spatial resolution of 100 m[1]. Raw observations are converted to scaled surface temperatures by the USGS, subsampled to 30 m resolution.

A total of 59 images from the years 2019–2022 were selected for inclusion in the study. Selection criteria are based on cloud-free skies and lack of other masking features (such as fog or smoke); satellite path and frame number were not considered. Images were downloaded from the USGS Earth Explorer website, imported into ESRI ArcGIS Pro, clipped to the AOI, and finally scaled and converted to degrees Celsius (°C) using the formula published by the USGS[2], where T is the temperature in degree Celsius and D is the pixel value of the raster at the point (x,y).

$$T_{x,y} = \left((D_{x,y} * 0.00341802) + 149\right) - 273.15 \quad (1)$$

The width of the bridge deck in the sampling area is less than the 100 m native pixel resolution of the Landsat 8/9 TIRS. In order to exclude pixels where average temperature includes both water and bridge measurements, a sampling line was drawn approximately 250 m upstream of the Samuel de Champlain bridge, between the bridge and the adjacent ice control structure, and sampling points upstream of each bridge pier were drawn along the line. Water surface temperatures were extracted at these sampling points. A temperature measurement was also taken at the west abutment of the bridge, which is fully located onshore. Figure 4 illustrates such temperature measurements for each selected pier. Pier W26, which is in very shallow water, indicates higher and lower temperatures than the other piers. We observe in multispectral imagery that landfast ice forms around this pier in wintertime, and the sub-freezing temperatures observed in TIRS imagery concur with these observations.

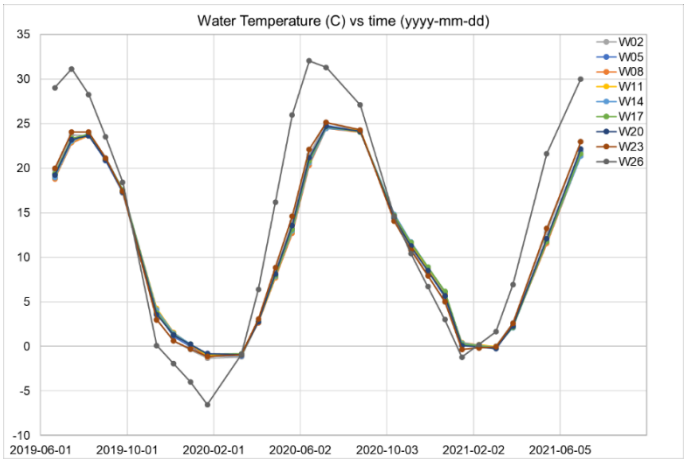

Figure 4. Water temperature measured by satellite for each selected pier over time.

[1] https://www.usgs.gov/media/images/landsat-8-band-designations

[2] https://www.usgs.gov/faqs/how-do-i-use-scale-factor-landsat-level-2-science-products

Multi-temporal PS-InSAR Analysis of radar satellite imagery

The RADARSAT-2 SLA12 descending stack was selected to perform the InSAR analysis [3], which provided reduced undesired radar effects and high sensitivity to deformations in the longitudinal direction of the bridge. This stack of images consists of 26 scenes acquired typically every 24 days from June 21, 2019 (10 days before the bridge's official opening to traffic), to July 4, 2021 (two years later). It has a typical footprint of 21.5 km in the range direction and 9.5 km in the azimuth direction. The SLA12-D stack characteristics include an incidence angle of 39° (from the vertical), a ground-range resolution of 2.5 m, and an azimuth resolution of 0.8 m (i.e., along the satellite track from north to south). Ambient temperature measurements at times of satellite passes were obtained from Environment and Climate Change Canada, which consisted of hourly temperature readings from the local Montreal/St-Hubert weather station. Temperature measurements were extracted at 6:00 AM local time (or 11:00 UTC). These ambient temperatures were used to estimate the thermal sensitivity coefficients for each InSAR target measured over the bridge.

InSAR is a remote sensing technique in which the amplitude and phase of two complex radar images acquired at two different times are combined to measure deformation over large geographic areas at pixel resolutions down to the meter scale. Multiple processing techniques exist to exploit mature stacks of SAR images to detect surface changes at the millimeter scale [4].

The Persistent Scatterer (PS) InSAR (or PSI) technique was used to analyze target phase quality using a spatially differential method, i.e., comparing the phase history of each target to that of its neighbors in order to identify the subset of spatial targets with high-quality phase. PSI is expected to produce its best results over highly-coherent urban areas with a high density of manmade structures and little to no vegetation. With a sufficient number of persistent scatterers (PS), a dense geodetic network can be formed, allowing accurate deformation observations at small scales. PSI has two main steps [3,5]: (i) Identify coherent targets (i.e., those with sufficient phase quality); and (ii) Estimate the deformation time history for each coherent target.

Figure 5 illustrates the line-of-sight (LOS) thermal displacement sensitivity averaged over the monitored period covering the Samuel de Champlain Bridge. The dataset shows an overall variation in the line-of-sight (including vertical and east-west horizontal components) along the bridge and appears to be in agreement with the expected thermal displacements of the different spans along the longitudinal axis of the bridge [1].

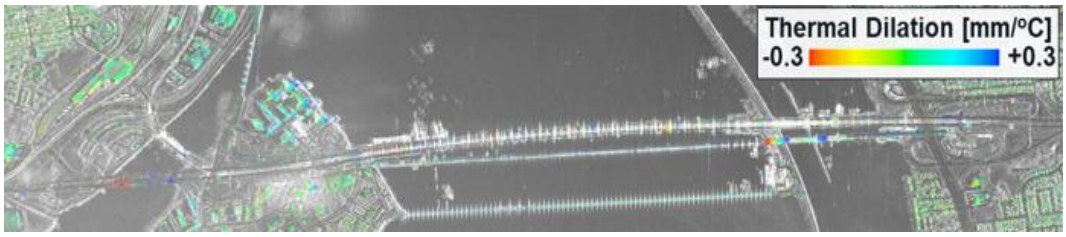

Figure 5. LOS thermal displacement sensitivity for the SLA12 descending stack over the Samuel de Champlain Bridge and surroundings [3].

RESULT ANALYSIS

This section seeks to find correlations between structural deformation data from the InSAR analysis and environmental data obtained from multispectral satellite imagery. For this, processed displacement data points similar to those illustrated in Figure 5 were imported into QGIS, clipped to the bridge deck areas over the piers, averaged for each pier, and compared to water depth and water temperature data collected for each pier and time of image acquisition.

Effect of Ambient Air and Water Temperature

Figure 6 illustrates the relation between the LOS displacement and the ambient air temperature measured at each selected pier. The datasets from ambient water temperature also gave very similar results. Some interesting observations include:

- Strong dependency of the LOS displacement (with an incidence angle of 39° from the vertical) with the ambient temperature (as normally expected);
- Most piers experienced negative displacement (down-west) with decreasing temperature, while the opposite displacement (up-east) was found for Piers W08 and W26. This is explained by the structural connection details between the supported spans at the piers and which direction thermal expansion is allowed to occur by design;
- Different amplitudes of LOS displacement with ambient temperature were observed for different piers (to be explained below).

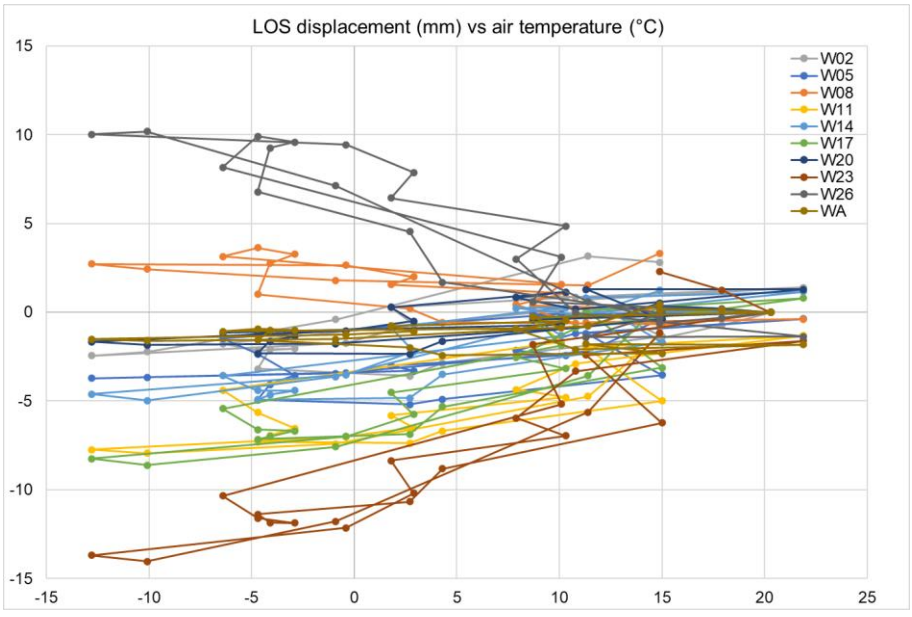

Figure 6. LOS displacement for each selected pier as a function of ambient air temperature measured at the Montreal/St-Hubert weather station.

Effect of Water Depth and Current Flow

Figure 7 illustrates the LOS displacements measured over the piers in relation to the water depths measured near the piers. With the exception of some measurement points over Pier W23 (discussed below), one can observe a general trend indicating an increase in the LOS displacement with a proportional increase in water depth. Acknowledging both horizontal (east-west) and vertical (up-down) components of the LOS measurement [1], this observation can be explained by the longer length of the piers in deeper water that can result in (i) bending leading to larger lateral (horizontal) deformations, and (ii) larger axial expansion/contraction observed at the top of the piers. Note that the LOS displacements discussed here are relatively small, with displacement values up to approximately 10 mm (including both vertical and horizontal components). As observed above in Figure 6, the different amplitudes of LOS displacement experienced by the different piers can be explained by the varying pier lengths/water depths along the bridge.

Other effects

Other sets of InSAR data were investigated to find whether they can be affected by water depth and current flow. These sets of data included displacement velocity (mm/year), thermal displacement sensitivity (mm/°C), temporal coherence (expressing the quality/reliability of the InSAR measurements on a scale of 0 to 1), and height (m) of InSAR measurements. Of these parameters, only the thermal sensitivity (averaged over the 2-year monitoring period) seemed to be affected by an environmental parameter, which is water depth (Fig. 8). This supports the results in Figure 7 where LOS displacements (at least the thermal component) at the piers appeared to be influenced by water depth, with the outlier of W23 again. The unusual results at Pier W-23 are thought to be related to construction activity and to the presence of landfast ice around the pier from December 2020 to March 2021. Both the construction activity, confirmed by the bridge authority, and the landfast ice extent are visible in the multispectral images.

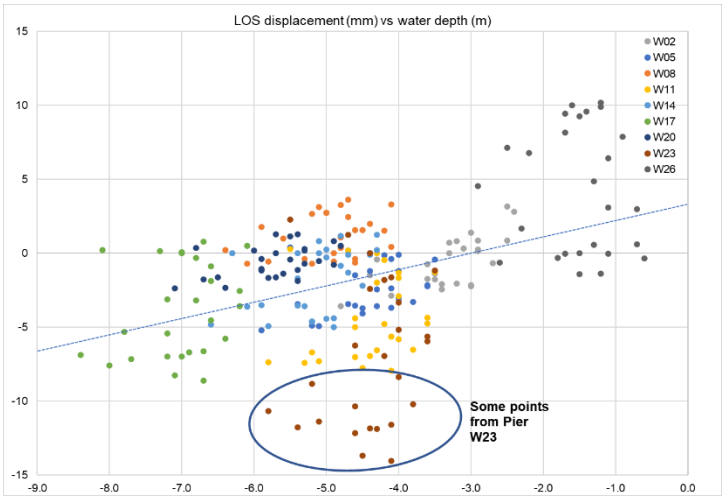

Figure 7. LOS displacement as a function of water depth at the piers (all piers confounded).

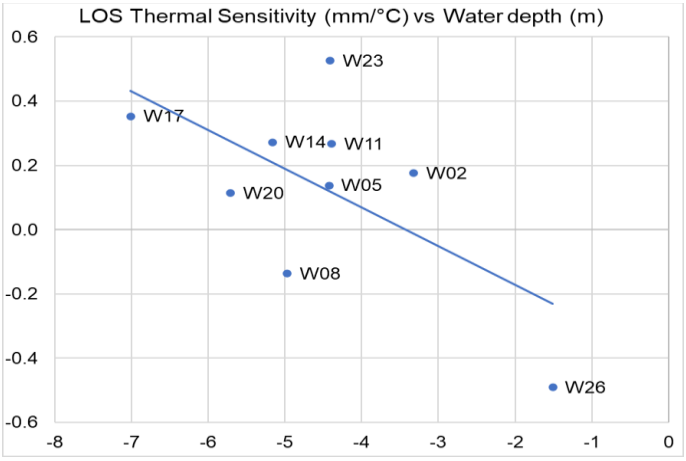

Figure 8. LOS displacement as a function of water depth at piers (all piers confounded).

CONCLUSIONS

This paper presented the preliminary findings of a study in which time series of InSAR displacement observations at nine selected piers of the Samuel de Champlain Bridge were compared to ambient air temperature, water depth, water surface temperature, and relative current flow obtained from multispectral satellite imagery. The main findings are as follows:

- Strong dependency of LOS displacement on ambient air temperature (as expected);
- Medium dependency of LOS displacement on water depth due to pier length;
- Medium dependency of LOS thermal displacement sensitivity on water depth.

ACKNOWLEDGMENTS

The authors wish to acknowledge the joint financial contribution of Transport Canada, Infrastructure Canada, and the National Research Council Canada.

REFERENCES

1. Cusson, D., I. Ozkan, J. Hiedra Cobo, F. Greene Gondi, H. Stewart. 2022. “Satellite-based Bridge Monitoring – Validation Case Study on the new Samuel the Champlain Bridge in Montréal Canada,” 11th Intl. Conference on Short & Medium Span Bridges, Toronto, Canada, July 19-22, 8 p.
2. Stewart, H., R. Simpson, A. Peach, D. Millar, D. Cusson, S. Anderson. 2022. “Optical-band satellite remote sensing of river turbulent and flow features to assist in structural health monitoring of bridge stability”, 11th International Conference on Structural Health Monitoring of Intelligent Infrastructure, August 8-12, Montreal, QC, Canada, 4 p.
3. MDA Geospatial Services. 2021. “InSAR Analysis of Satellite Imagery Over Bridge Sites: Champlain Bridge, Montreal (QC),” Technical Report 617-21-260-02 for NRC, Sept. 30, 40 p.
4. Marinkovic, P., G. Ketelaar, F. Van Leijen, and R. Hanssen. 2007. “InSAR Quality Control - Analysis of Five Years of Corner Reflector Time Series.” 5th Intl. Workshop on ERS/Envisat SAR Interferometry, Frascati, Italy, 26-30 November.
5. Ferretti, A., A. Monti-Guarnieri, C. Prati, F. Rocca, and D. Massonnet. 2007. “InSAR Principles: Guidelines for SAR Interferometry Processing & Interpretation,” European Space Agency Publication TM-19, European Space Agency, Noordwijk, The Netherlands, 48 p.